RARE METALS
Vol. 29, No. 2, Apr 2010, p. 180
DOI: 10.1007/s12598-010-0031-5

Fabrication of gold nanoparticles with different morphologies in HEPES buffer

CHEN Rong[a, b], WU Jiliang[a], LI Hui[a], CHENG Gang[a], LU Zhong[a], and CHE Chi-Ming[b]

[a] *School of Chemical Engineering and Pharmacy, Key Laboratory for Green Chemical Process (Ministry of Education), Hubei Key Lab of Novel Reactor and Green Chemical Technology, Wuhan Institute of Technology, Wuhan 430074, China*

[b] *Department of Chemistry and the HKU-CAS Joint Laboratory on New Materials, The University of Hong Kong, Pokfulam Road, Hong Kong, China*

Received 26 April 2009; received in revised form 15 May 2009; accepted 20 May 2009

Abstract

Gold nanoparticles with different morphologies, such as spindle, octahedron, and decahedron were obtained by using different molar ratios of $HAuCl_4$/HEPES in the presence and absence of surfactants at room temperature. These nanoparticles were characterized by X-ray diffraction (XRD), transmission electron microscopy (TEM), high-resolution transmission electron microscopy (HRTEM), scanning electron microcopy (SEM), energy-dispersive X-rays analysis (EDX), and selected area electron diffraction (SAED). The kinetics of the formation of gold nanoparticles in HEPES buffer was studied by UV-visible spectrophotometer. The formation of gold nanoparticles was strongly dependent on the concentration of HEPES and pH value. The surfactants play a crucial role in the size and shape controlled synthesis of gold nanoparticles.

Keywords: inorganic chemistry; gold nanoparticle; HEPES buffer; surfactant

1. Introduction

Metal nanoparticles display fascinating electronic, optical, and biological properties as a consequence of their dimensions [1-5]. Synthesis of metal nanostructure has been an active research area for many decades. Much effort has been devoted to application studies of these nanoparticles, especially in biological systems [6-11]. Applications of gold nanoparticles include biological markers, DNA sensors [12], molecular recognition systems [13], and nanoscale electronics14]. The interaction of colloidal gold nanoparticles with DNA, protein (enzymes), and virus, as well as the study on the application of gold nanoparticles, gold nanoparticles-bound oligonucleotides, and gold nanoparticles-peptide complexes as targeting spectroscopic enhancer or linker have received much attention [15-21]. Due to these potential applications, it is crucial to prepare gold nanoparticles with high monodispersity, purity, and amenable to biomolecule attachment.

In literature, there are numerous physical and chemical methods of generating gold nanoparticles [22-25]. Among the reported methods, the reduction of $HAuCl_4$ by using reducing agents such as sodium citrate, sodium borohydride, hydrazine, and dimethyl formamide is the common used method for preparation of gold nanoparticles. As the potential environmental and biological risks of these chemicals, an environment friendly "green chemistry" has been proposed for the preparation of metal nanoparticles. Recently, the "green" synthesis of gold and silver nanoparticles at room temperature using aqueous solutions of the ionic polymers was presented. Different types of fungi and bacteria have been found to work up with metal salts into elemental metal [26-28]. The production of gold nanoparticles and nanoflowers by $HAuCl_4$ or $NaAuCl_4$ in the presence of Good's buffers [29-31] was also reported. Silver nanoparticles also have been synthesized in HEPES buffer [2]. As the application performance of metal nanoparticles depends mainly on their size, shape, and structure, herein, the rapid formation of gold nanoparticles with different morphologies in HEPES buffer was reported.

2. Experimental

2.1. Synthesis of gold nanoparticles

Hydrogen tetrachloroaurate(III) trihydrate ($HAuCl_4 \cdot 4H_2O$) was purchased from Aldrich, poly(ethylene glycol) (PEG,

Corresponding author: CHEN Rong **E-mail:** rchenhku@hotmail.com

with average M_w of 4600), poly(vinylpyrrolidone) (PVP, with average M_w of 10000), sodium borohydride, and 4-(2-hydroxyethyl)-1-piperazineethane-sulfonic acid (HEPES) were purchased from Sigma-Aldrich Chemical Company. Sodium citrate and (*N*-hexadecyl) trimethylammonium bromide (CTAB) were purchased from Lancaster.

$HAuCl_4$ solution (10 mmol/L, 1 mL) was mixed with HEPES buffer (50 mmol/L, 9 mL, pH 7.4) with vigorous stirring. After several minutes, the colorless solution changed to a red color, indicating formation of gold nanoparticles (sample 1). Gold nanoparticles also have been synthesized by the different molar ratios of $HAuCl_4$/HEPES (1:10, 1:20, 1:30, and 1:40). Under identical condition, gold nanoparticles were also prepared in the presence of 0.1 mol/L CTAB (sample 2), 1 mmol/L PVP (sample 3), and 1 mmol/L PEG (sample 4), respectively.

100 mmol/L HEPES buffer (pH 7.4) of 2.8 mL was put into quartz colorimetric utensil, and recorded the UV-vis spectra on the Perkin Elmer Lambda 35 spectrophotometer each 15 s, starting from the addition of 0.2 mL $HAuCl_4$ (10 mmol/L) to HEPES buffer, until no obvious spectral changes. The UV-vis spectra were recorded under the same conditions when the concentration of HEPES buffer is 50 mmol/L and 10 mmol/L, respectively.

2.2. Characterization

The XRD spectra were recorded with Philips PW1830 powder X-ray diffractometer. UV-visible absorption spectra were recorded using Varian cary-50 and Perkin Elmer Lambda 35 spectrophotometer, and TEM images were taken with JEOL JEM-2000 transmission electron microscopy (accelerating voltage of 200 kV) and Philips Tecnai 20 equipped with Oxford INCAx-sight EDX attachment (accelerating voltage of 200 kV). Measurements of pH values were made with a Corning 440 pH meter equipped with a micro-combination electrode (Aldrich), calibrated with standard buffer solutions. Size distribution of nanoparticles was measured by Zetasizer 3000 HS (Malven Instruments, UK).

3. Results

3.1. XRD analysis

The powder X-ray diffraction (XRD) patterns taken from a larger quantity of samples revealed that the gold nanoparticles generated in HEPES buffer existed predominantly in face-center-cubic (fcc) phase. As depicted in Fig. 1, the presence of intense peaks corresponding to 2θ values of (111), (200), (220), and (311) in the powder X-ray diffraction pattern agrees with those values reported in literature (JCPDS No.04-0784). Gold nanoparticles were also obtained in the mixture of different molar ratio of gold salt and HEPES buffer (from (a) to (d): 1:10, 1:20, 1:30, and 1:40, inset of Fig. 1). It confirmed that the gold nanoparticles could be obtained under different molar ratios of $HAuCl_4$/HEPES.

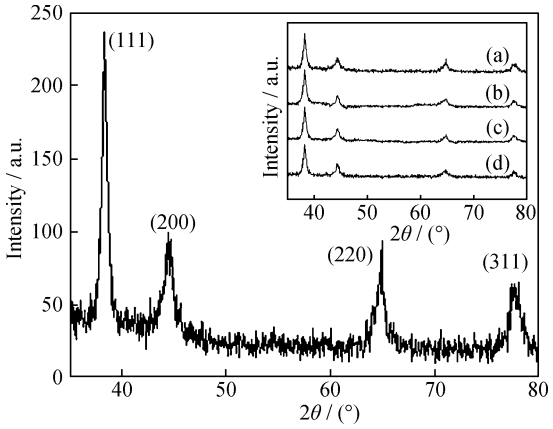

Fig. 1. Powder XRD spectra of gold nanoparticles obtained from HEPES buffer (sample 1) (the $HAuCl_4$/HEPES molar ratio is 1:45). Patterns (a), (b), (c), and (d) in the insert correspond to $HAuCl_4$/HEPES molar ratios: 1:10, 1:20, 1:30, and 1:40, respectively.

3.2. UV-visible analysis

By UV-visible spectrophotometry, it was found that the gold nanoparticles (sample 1) were formed within 5 min, and no spectral changes were observed after 1 h, indicating that formation of the gold nanoparticles was completed within 1 h when the concentrations of $HAuCl_4$ and HEPES were 1 mmol/L and 50 mmol/L, respectively (Fig. 2(a)). However, the maximum absorption peaks of gold nanoparticles varied slightly with different molar ratios of $HAuCl_4$/HEPES, indicative of only a size variation of gold nanoparticles (Fig. 2(b)). As shown in Figs. 2(c-e), the speed of formation of gold nanoparticles decreased with the increasing of the molar ratio of $HAuCl_4$/HEPES in the presence of 0.67 mmol/L $HAuCl_4$. (Figs. 2(c-e) correspond to $HAuCl_4$/HEPES ratios of 1:140, 1:70, and 1:14, respectively).

3.3. TEM, HRTEM, SEM and SAED analysis

The transmission electron microscopy (TEM) images of the gold nanoparticles prepared from HEPES buffer (pH 7.4) in the absence of any surfactant (sample 1) are shown in Fig. 3. The gold nanoparticles are uniformly distributed with particle size ranging from 5 to 30 nm and an average diameter 18±0.6 nm. A histogram shows the size distribution of the gold nanoparticles (sample 1) (inset of Fig. 3(a)). Interestingly, different morphologies of the gold nanoparticles were found in the sample. Most nanoparticles are spherical and some of them are spindle, as shown in the enlarged TEM

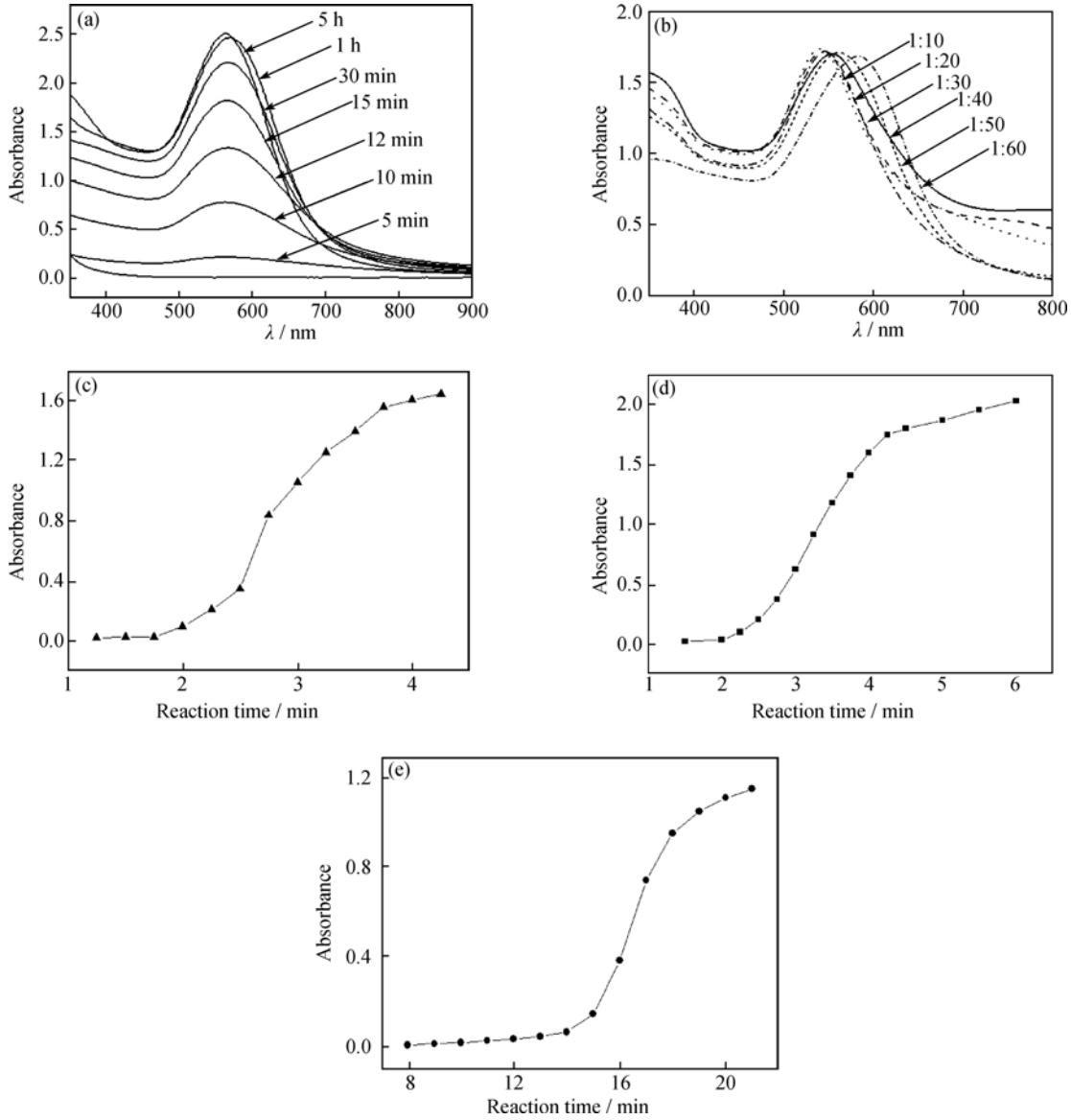

Fig. 2. (a) UV-vis absorption spectra of a solution mixture of $HAuCl_4$ and HEPES with a molar ratio of 1:40 (sample 1) recorded at different time intervals ([$HAuCl_4$] = 1 mmol/L); (b) UV-vis absorption spectra of gold nanoparticles obtained from HEPES buffer (sample 1) with different $HAuCl_4$/HEPES molar ratios (1:10, 1:20, 1:30, 1:40, 1:50, and 1:60), and the initial concentration of $HAuCl_4$ was 10 mmol/L and HEPES was 50 mmol/L; (c-e) The maximum absorption at 554 nm of gold nanoparticles at different times (Figs. 2(c-e) correspond to $HAuCl_4$/HEPES molar ratios of 1:140, 1:70, and 1:14, respectively, [$HAuCl_4$] = 0.67 mmol/L).

and high-resolution transmission electron microscopy (HRTEM) images of individual gold particles (inset of Figs. 3(a-b)). The clear lattice fringes of the spindle gold nanoparticles grow preferentially along [111] and [200] directions.

The corresponding SAED pattern of the selected area in Fig. 3(a) was shown in the inset of Fig. 3(b). It exhibits several diffraction ring patterns, which are characteristic of a polycrystalline structure. It is the sum of different single-crystallized gold nanoparticles due to each of them exhibiting a different orientation and crystal plane.

Gold nanoparticles with different morphologies and size were synthesized in the presence of different surfactants. Fig. 4 shows the scanning electron microscopy (SEM) images of gold nanoparticles prepared from HEPES buffer in the presence of CTAB (sample 2) at different magnifications. In the presence of CTAB, gold nanoparticles in different shapes including triangle, octahedron, and decahedron were found. The gold nanoparticles were further examined by the transmission electron microscopy (TEM) (Figs. 5(a-d)). A decahedral structure was clearly depicted in Fig. 5(b). Inset of Fig. 5(a) shows a SAED pattern of the gold nanoparticles, which exhibits several diffraction ring patterns, indicative of a polycrystallized structure.

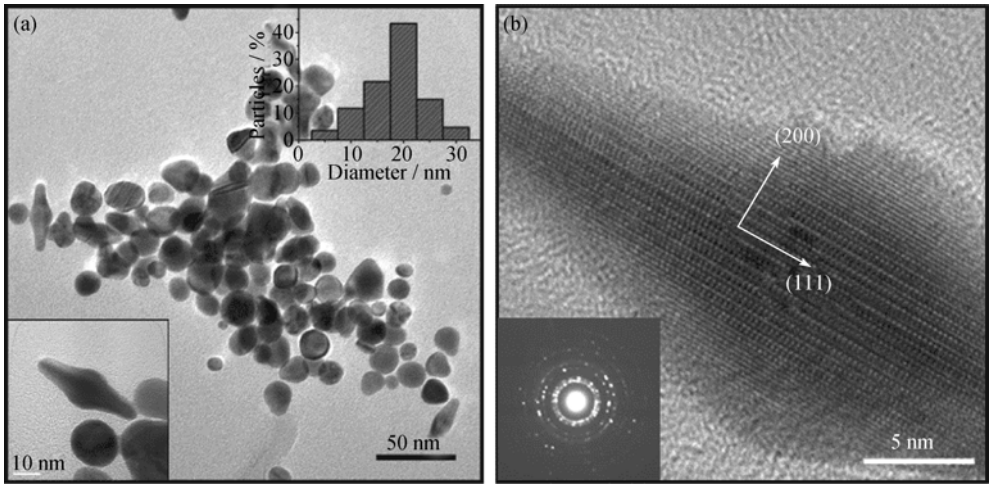

Fig. 3. (a) TEM images of gold nanoparticles prepared from HEPES buffer (sample 1), and the insets of (a) are the histogram of size distribution of the gold nanoparticles (sample 1) and the corresponding enlarged TEM image of selected nanoparticles, respectively; (b) HRTEM image of individual gold nanoparticles, and the inset of (b) corresponds to the SAED pattern of selected area in (a).

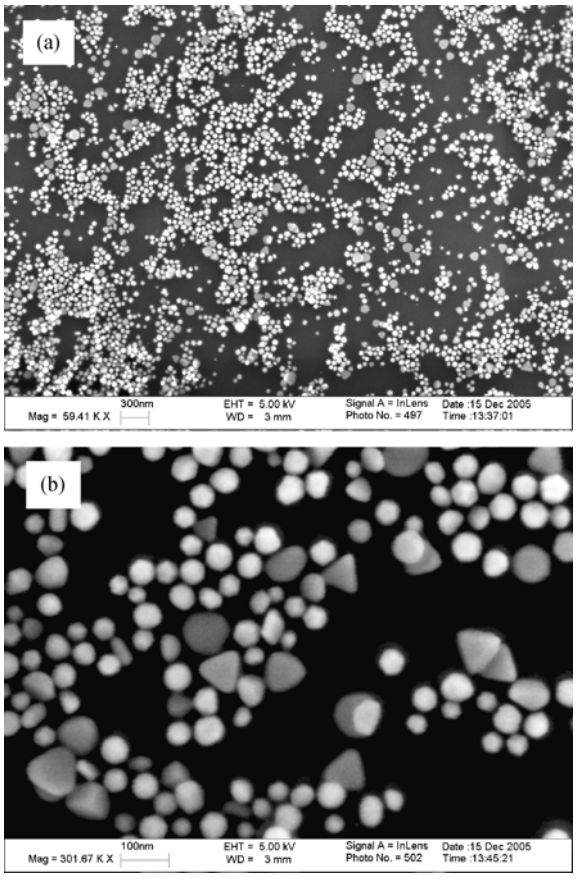

Fig. 4. SEM images of gold nanoparticles obtained from HEPES buffer in the presence of CTAB (sample 2) at different magnifications.

In the presence of PVP, only spherical gold nanoparticles were obtained in HEPES buffer. Figs. 5(e-f) showed the TEM images of gold nanoparticles prepared from HEPES buffer in the presence of PVP (sample 3). These nanoparticles are uniform with a diameter of 10 nm and well separated. This size distribution profile was shown in the inset of Fig. 5(f). The inset of Fig. 5(e) shows the SAED pattern of selected area of gold nanoparticles (sample 3), revealing several diffraction rings.

In the presence of PEG, gold nanoparticles with diameters of 20-50 nm were obtained (Fig. 5(g)). Interestingly, rod-like gold nanoparticles were found when the concentration of PEG was enhanced (5 mmol/L) under the same conditions (Fig. 5(h)). Insets of Figs. 5(g-h) show the SAED patterns of selected area of spherical and rod-like gold nanoparticles, indicative of their polycrystalline structures. No similar phenomenon was found when the concentrations of CTAB and PVP were increased.

4. Discussion

The selection of a proper buffer for studies on the chemistry and biochemistry of transition metals is very important. Many buffers provide a potential ligand for the metal ions. However, the Good's buffers including HEPES buffer have low affinities for transition-metal ions and are widely used in biological research. However, it was found that some of Good's buffers can give nitrogen-centered cation free radicals in the presence of Fe(II) [32] and can be oxidized by Cu(II) [33]. Recently, the research on the synthesis of gold nanoparticles by Good's buffers has been widely studied. Similar with the reported literature, this study proposes that HEPES buffer generates nitrogen-centered cationic free radicals in the presence of Au(III), leading to the formation of gold nanoparticles. In this work, gold nanoparticles with

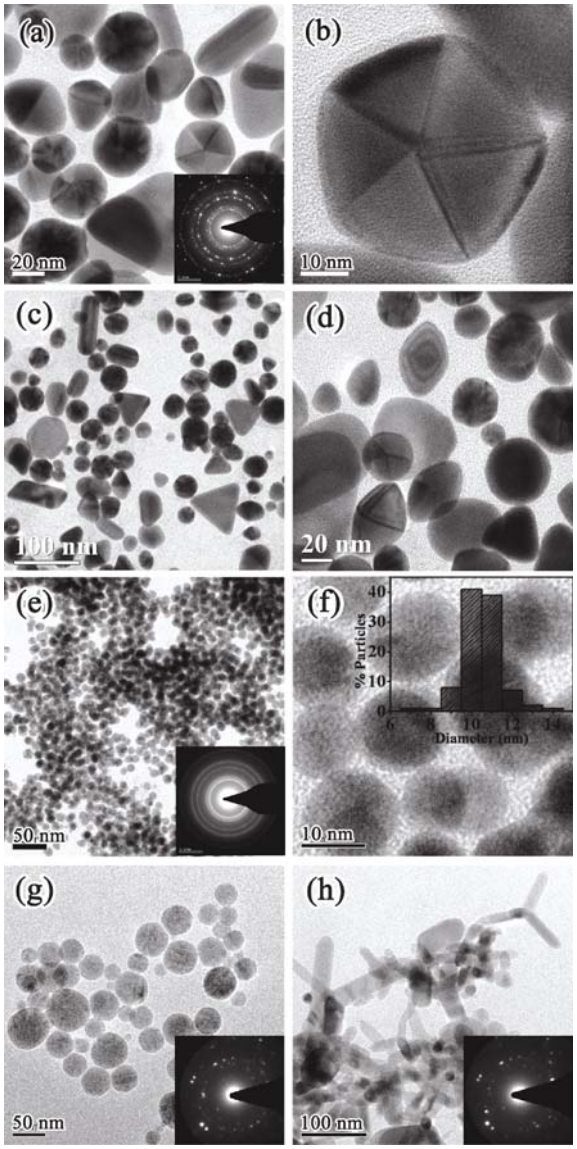

Fig. 5. TEM images of gold nanoparticles obtained from HEPES buffer in the present of different surfactants: CTAB (sample 2), (a-d); PVP (sample 3), (e-f); PEG (sample 4), (g-h). The insets of (a), (e), (g), and (h) show corresponding SAED patterns of gold nanoparticles, and the inset of (f) is the size distribution profile of gold nanoparticles obtained from HEPES buffer in the presence of PVP (sample 3).

different morphologies were formed within a few minutes by dissolving $HAuCl_4$ in HEPES buffer solution (pH 7.4) at room temperature, and no other reducing agents were needed. Compared to other reported methods of the formation of gold nanoparticles, this method is unique in which the reaction is fast (within minutes) even at room temperature. For the reduction of Au^{3+} to Au^0, piperazine as the functional group could be oxidized [30]. The formation of gold nanoparticles was affected by the reaction conditions such as the concentration of HEPES and pH value. For example, when the pH was adjusted to 5.4, no gold nanoparticles were found even after several days (dates are not shown). Figs. 2(c-e) show that the formation of gold nanoparticles was affected by molar ratios of $HAuCl_4$/HEPES. In the presence of same amount of $HAuCl_4$, the formation speed of gold nanoparticles was increased with the increasing of the concentration of HEPES. When the concentration of HEPES is 100 mmol/L and 10 mmol/L, absorption at 554 nm will not changed within 4 and 20 min, respectively.

In recent studies, soluble polymer or surfactant was reported as capping agents for the preparation of metal nanoparticles [34-35]. In the presence of CTAB, which is a cationic surfactant, gold ion would not be absorbed on micelle. It was suggested that gold nanoparticles were capped by CTAB molecules. CTAB molecules might be present on the surface of metal nanoparticles in two different forms, as suggested previously [34]. As the surface of metal atoms usually carries negative charges, the inner layer of CTAB is bound to the particle surface via the headgroups and is connected to the outer layer, whose headgroups are in the aqueous solution, through hydrophobic interaction [34]. When HEPES buffer was added to the CTAB-Au^{3+} solution, the color of solution changed from yellow to red, suggesting that the Au^{3+} complex was reduced to Au^0. Compared with ascorbic acid, which is a weak reducer, HEPES is a moderate reducer, and it is very important for the growth of particles with different shapes [36]. Gold decahedral nanostructure, which consists of five equal tetrahedral subunits bound together by five twinned (111) planes and five twinned axes, has been observed (Fig. 5(b)). Triangular, multiangular, octahedral crystallites and octahedral structures also have been obtained in the condensed CTAB-capped phase (Fig. 4(b) and Figs. 5(a-d)). It was very similar with the proposed mechanism of particle growth in Refs. [36-37]. The effect of CTAB concentration on the size and shape of gold nanoparticles has also been investigated. The size of gold nanoparticles was not significantly changed when the concentration of CTAB varied from 100 to 1 mmol/L. Hence, CTAB acted as a capping agent in controlling the size of gold nanoparticles.

Interestingly, no variation in the morphology of gold nanoparticles was observed in the presence of PVP and PEG. Only spherical gold nanoparticles were obtained from HEPES buffer in the presence of PVP and PEG. The surfactant did not play a role in affecting the morphology of gold nanoparticles. In fact, $AuCl_4^-$ can form complex with CTAB in aqueous solution to generate aqueous foams by bubbling the solution, and $AuCl_4^-$ in the foam and its subsequent reduction would result in the formation of gold particles having nanostructure and variable morphology [38]. The shape-controlled synthesis of silver and gold nanoparti-

cles in the presence of PVP was reported in Ref. [39]. It was suggested that the morphology and dimensions of metal nanoparticles were strongly affected by the molar ratio between the repeating unit of PVP and metal salt. Selective absorption of PVP on various crystallographic planes of silver also plays a major role in determining the product morphology.

PEG is a nonionic polymer containing hydrophilic –O– and hydrophobic $–CH_2–CH_2–$ groups; it is not a good stabilizing agent compared to CTAB and PVP in the formation of gold nanoparticles in HEPES buffer. PEG can extend to a long chain to facilitate complexing with $AuCl_4^-$ ions. PEG would act as a nucleus for aggregation. Hydrogen bonding between the –O– group on PEG and the water in the aqueous solution is anticipated. This bonding is instructive to the formation of $AuCl_4$-PEG complexes, leading to its extension in solution. Thus, PEG can curl or extend to form a polymer chain in aqueous solution, providing a useful microenvironment to the formation of rod-like nanostructure. Up to now, the growth mechanism of shape-controlled synthesis of nanoparticles in different surfactants remains poorly understood.

5. Conclusions

A method for the preparation of gold nanoparticles from $HAuCl_4$ in HEPES buffer without addition of other reducing agents is described. This protocol is simple, quick, and environment friendly. These gold nanoparticles are stable and comparable in size and polydispersity to those produced using the reported other methods. More interestingly, the majority of the gold particles has intriguing shapes, such as spindle, octahedral, and decahedral structures in the present or absence of surfactants. The fabrication of gold nanoparticles was strongly affected by the molar ratio of $HAuCl_4$ to HEPES and pH value.

Acknowledgements

Authors acknowledge the financial supports from the Program for Excellent Talents of the Department of Education of Hubei Province, China (No. Q20081504) and the Area of Excellence Scheme administered by the University Grant Committee and the University of Hong Kong (No. AoE/ P-10/ 01).

References

[1] Shipway A.N., Katz A., and Willner I., Nanoparticle arrays on surfaces for electronic, optical, and sensor applications, *Chem. Phys. Chem.*, 2000, **1** (1): 18.

[2] Sun R.W.Y., Chen R., Chung N.P.Y., Ho C.M., Lin C.L.S., and Che C.M., Silver nanoparticles fabricated in Hepes buffer exhibit cytoprotective activities toward HIV-1 infected cells, *Chem. Commun.*, 2005, **40**: 5059.

[3] Milliron D.J., Hughes S.M., Cui Y., Manna L., Li J., Wang L.W., and Alivisatos A.P., Colloidal nanocrystal heterostructures with linear and branched topology, *Nature*, 2004, **430**: 190.

[4] Liz-Marzán L.M., Tailoring surface plasmons through the morphology and assembly of metal nanoparticles, *Langmuir*, 2006, **22** (1): 32.

[5] Lok C.N., Ho C.M., Chen R., He Q.Y., Yu W.Y., Sun H., Tam P.K.H., Chiu J.F., and Che C.M., Silver nanoparticles: partial oxidation and antibacterial activities, *J. Biol. Inorg. Chem.*, 2007, **12**: 527.

[6] Elghanian R., Storhoff J.J., Mucic R.C., Letsinger R.L., and Mirkin C.A., Selective colorimetric detection of polynucleotides based on the distance-dependent optical properties of gold nanoparticles, *Science,* 1997, **277**: 1078.

[7] Chan W.C.W. and Nie S., Quantum dot bioconjugates for ultrasensitive nonisotopic detection, *Science,* 1998, **281**: 2016.

[8] Han M., Gao X., Su J.Z., and Nie S., Quantum-dot-tagged microbeads for multiplexed optical coding of biomolecules, *Nat. Biotechnol.,* 2001, **19**: 631.

[9] Mirkin C.A., Letsinger R.L., Mucic R.C., and Storhoff J.J., A DNA-based method for rationally assembling nanoparticles into macroscopic materials, *Nature,* 1996, **382**: 607.

[10] Schultz S., Smith D.R., Mock J.J., and Schultz D.A., Single-target molecule detection with nonbleaching multicolor optical immunolabels, *Proc. Natl. Acad. Sci. USA,* 2000, **97** (3): 996.

[11] Bruchez Jr M., Moronne M., Gin P., Weiss S., and Alivisatos A.P., Semiconductor nanocrystals as fluorescent biological labels, *Science*, 1998, **281**: 2013.

[12] Liu T., Tang J., and Jiang L., The enhancement effect of gold nanoparticles as a surface modifier on DNA sensor sensitivity, *Biochem. Biophys. Res. Commun.*, 2004, **313** (1): 3.

[13] Tshikhudo T.R., Demuru D., Wang Z., Brust M., Secchi A., Arduini A., and Pochini A., Molecular recognition by calix[4]arene-modified gold nanoparticles in aqueous solution, *Angew. Chem. Int. Ed.,* 2005, **44** (19): 2917.

[14] Huang D., Liao F., Molesa S., Redinger D., and Subramanian V., Plastic-compatible low resistance printable gold nanoparticle conductors for flexible electronics, *J. Electrochem. Soc.*, 2003, **150** (7): 412.

[15] Niemeyer C.M. and Dr P.D., Nanoparticles, proteins, and nucleic acids: biotechnology meets materials science*, Angew. Chem. Int. Ed.,* 2001, **40** (22): 4128.

[16] Hill H.D., Macfarlane R.J., Senesi A.J., Lee B., Park S.Y., and Mirkin C.A., Controlling the lattice parameters of gold nanoparticle FCC crystals with duplex DNA linkers, *Nano Lett.*, 2008, **8** (8): 2341.

[17] Tabata M., Habib A. and Watanabe K., DNA cleavage by good's buffers in the presence of Au(III), *Bull. Chem. Soc. Jpn.*, 2005, **78**: 1263.

[18] Nicewarner-Peña S.R., Raina S., Goodrich G.P., Fedoroff N.V., and Keating C.D., Hybridization and enzymatic extension of Au nanoparticle-bound oligonucleotides, *J. Am. Chem. Soc.*, 2002, **124** (25): 7314.

[19] Tkachenko A.G., Xie H., Coleman D., Glomm W., Ryan J., Anderson M.F., Franzen S., and Feldheim D.L., Multifunctional gold nanoparticle-peptide complexes for nuclear targeting, *J. Am. Chem. Soc.,* 2003, **125** (16): 4700.

[20] Dragnea B., Chen C., Kwak E.S., Stein B., and Kao C.C., Gold nanoparticles as spectroscopic enhancers for *in vitro* studies on single viruses, *J. Am. Chem. Soc.,* 2003, **125** (21): 6374.

[21] Bowman M.G., Ballard T.E., Ackerson C.J., Feldheim D.L., Margolis D.M., and Melander C., Inhibition of HIV fusion with multivalent gold nanoparticles, *J. Am. Chem. Soc.* 2008, **130** (22): 6896.

[22] Schmid G. and Corain B., Nanoparticulated gold: syntheses, structures, electronics, and reactivities, *Eur. J. Inorg. Chem.,* 2003, (17): 3081.

[23] García-Serrano J., Pal U., Herrera A.M., Salas P., and Ángeles-Chávez C., One-step "green" synthesis and stabilization of Au and Ag nanoparticles using ionic polymers, *Chem. Mater.*, 2008, **20** (16): 5146.

[24] Link S., Wang Z.L., and EI-Sayed M.A., Alloy formation of gold-silver nanoparticles and the dependence of the plasmon absorption on their composition, *J. Phys. Chem. B,* 1999, **103** (18): 3529.

[25] Okitsu K., Yue A., Tanabe S., Matsumoto H., and Yobiko Y., Formation of colloidal gold nanoparticles in an ultrasonic field: control of rate of gold (III) reduction and size of formed gold particles, *Langmuir*, 2001, **17** (25): 7717.

[26] Mukhejee P., Ahmad A., Mandal D., Senapati S., Sainkar S.R., Khan M.I., Ramani R., Parischa R., Ajayakumar P.V., Alam M., Sastry M., and Kumar R., Bioreduction of $AuCl_4^-$ ions by the fungus, *Verticillium sp.* and surface trapping of the gold nanoparticles formed, *Angew. Chem. Int. Ed.*, 2001, **40** (19): 3585.

[27] Sugunan A., Melin P., Schnürer J., Hilborn J.G., and Dutta J., Nutrition-driven assembly of colloidal nanoparticles: growing fungi assemble gold nanoparticles as microwires, *Adv. Mater.*, 2007, **19** (1): 77.

[28] He S., Guo Z., Zhang Y., Zhang S., Wang J., and Gu N., Biosynthesis of gold nanoparticles using the bacteria *Rhodopseudomonas capsulata*, *Mater. Lett.,* 2007, **61** (18): 3984.

[29] Habib A., Tabata M., and Wu Y.G., Formation of gold nanoparticles by Good's buffers, *Bull. Chem. Soc. Jpn.*, 2005, **78**: 262.

[30] Xie J., Lee J.Y., and Wang D.I.C., Seedless, surfactantless, high-yield synthesis of branched gold nanocrystals in HEPES buffer solution, *Chem. Mater.*, 2007, **19** (11): 2823.

[31] Jena B.K. and Raj C.R., Synthesis of flower-like gold nanoparticles and their electrocatalytic activity towards the oxidation of methanol and the reduction of oxygen, *Langmuir*, 2007, **23** (7): 4064.

[32] Grady J.K., Chasteen N.D., and Harres D.C., Radicals from Good's buffers, *Anal. Biochem.*, 1988, **173** (1): 111.

[33] Hegetschweiler K. and Saltman P., Interaction of copper(II) with *N*-(2-hydroxyethyl)piperazine-*N*'-ethanesulfonic acid (HEPES), *Inorg. Chem.*, 1986, **25** (1): 107.

[34] Wu S.H. and Chen D.H., Synthesis of high-concentration Cu nanoparticles in aqueous CTAB solutions, *J. Colloid Interface Sci.*, 2004, **273** (1): 165.

[35] Wiley B., Sun Y., Mayers B., and Xia Y., Shape-controlled synthesis of metal nanostructures: the case of silver, *Chem. Eur. J.*, 2004, **11** (2): 454.

[36] Cao C., Park S., and Sim S.J., Seedless synthesis of octahedral gold nanoparticles in condensed surfactant phase, *J. Colloid Interface Sci.*, 2008, **322** (1): 152.

[37] Robertson D., Tiersch B., Kosmella S., and Koetz J., Preparation of crystalline gold nanoparticles at the surface of mixed phosphatidylcholine-ionic surfactant vesicles, *J. Colloid Interface Sci.*, 2007, **305** (2): 345.

[38] Mandal S., Arumugam S.K., Adyanthaya S.D., Pasricha R., and Sastry M., Use of aqueous foams for the synthesis of gold nanoparticles of variable morphology, *J. Mater. Chem.* 2004, **14**: 43.

[39] Sun Y. and Xia Y., Shape-controlled synthesis of gold and silver nanoparticles, *Science*, 2002, **298**: 2176.